CHEMICAL ENGINEERING TRANSACTIONS
VOL. 39, 2014
A publication of AIDIC
The Italian Association of Chemical Engineering
www.aidic.it/cet
Guest Editors: Petar Sabev Varbanov, Jiří Jaromír Klemeš, Peng Yen Liew, Jun Yow Yong

ISBN 978-88-95608-30-3; **ISSN** 2283-9216
DOI: 10.3303/CET1439010

Optimum Energy Management in Smart Grids Based on Power Pinch Analysis

Damian Giaouris[a], Athanasios I. Papadopoulos[a], Panos Seferlis[b], Simira Papadopoulou[c], Spyros Voutetakis[a], Fotis Stergiopoulos[c], Costas Elmasides[d]

[a]Chemical Process and Energy Resources Institute, Centre for Research and Technology-Hellas, 57001 Thermi, Greece
[b]Department of Mechanical Engineering, Aristotle University of Thessaloniki, 54124 Thessaloniki, Greece
[c]Department of Automation Engineering, Alexander Technological Educational Institute of Thessaloniki, 57400 Thessaloniki, Greece
[d]Sunlight S.A., Xanthi, Greece
spapadopoulos@cperi.certh.gr

This work proposes a systemic approach to identify optimum power management strategies (PMS) in renewable energy smart-grids by using the Power Grand Composite Curves (PGCC) approach to adaptively adjust the system operation in short-term power requirements. This is approached by a) using the PGCC to target the optimum power requirements for the subsequent time interval and b) then adjusting the system PMS in the current time-interval to meet the identified target by the end of this interval. First the system PGCC is developed for the subsequent time interval, indicating the external non-renewable input required to satisfy the expected power demands. An appropriate shift in the PGCC sets a target of the minimum power inventory needed by the end of the current interval to completely avoid the use of non-renewable power input in the subsequent interval. The development of this power inventory is then approached in the current interval by identifying the PMS that best satisfies this target. The method is illustrated through a hybrid smart grid considering multiple renewable sources and storage options.

1. Introduction

Smart grids based on renewable energy sources (RES) are receiving increased attention worldwide as they required to support isolated and non-grid connected applications. To address the intermittent nature of largely unpredictable environmental phenomena, such systems transform RES into dependable power flows by simultaneous utilisation of different types of conversion equipment and storage media (e.g., PV panels, wind generators, chemical accumulators, hydrogen and so forth). The resulting infrastructures combine multiple subsystems that need to operate efficiently while satisfying power demands ideally based on RES. This is generally approached through the development of power management strategies (PMS) that typically account for decisions regarding the appropriate instance to activate or deactivate different subsystems, the duration of operation of a particular subsystem, the amount or type of energy carrier to use and so forth (Giaouris et al., 2013). Conventional grids mainly utilize a pre-specified PMS repeated throughout the cyclic system operation, which is inefficient in view of the variability observed in RES. An approach involving the recurrent identification and implementation of a new PMS within short time intervals would be more efficient. This involves numerous potential decision combinations resulting from the need to frequently select an optimum system configuration from several available PMS. A systemic method is required which is able to identify optimum performance targets, subsequently interpreted as appropriately fitted operating realizations.
The recently proposed Power Pinch Analysis (Wan Alwi et al., 2012a) is one such method, allowing the investigation of complex energy systems based on the identification of insights pointing towards optimum decisions. Focusing on hybrid power systems the method utilizes Composite Curves (Wan Alwi et al., 2012b) or Grand Composite Curves (Bandyopadhyay, 2011) similarly to the traditional Heat Pinch

Please cite this article as: Giaouris D., Papadopoulos A.I. , Seferlis P. , Papadopoulou S., Voutetakis S., Stergiopoulos F., Elmasides C., 2014, Optimum energy management in smart grids based on power pinch analysis, Chemical Engineering Transactions, 39, 55-60 DOI:10.3303/CET1439010

(Klemeš, 2013). However the associated sink and source streams are plotted in power versus time diagrams. The graphical power pinch analysis method takes the form of numerical tools such as the Power Cascade Analysis (PoCA) and Storage Cascade Table - SCT (Rozali et al., 2013), while the numerical tools are extended to consider power losses (Wan Alwi et al., 2012). The method is applied in the optimisation of a pumped hydro-storage system (Rozali et al., 2013a), while it is also extended to address the optimal sizing of hybrid systems (Rozali et al., 2013b). Recent work (Ho et al., 2013) proposed the stand-alone hybrid system Power Pinch Analysis method (SAHPPA) which employs new ways of utilising the demand and supply Composite Curve methods. Power Pinch methods have also taken the form of a MILP-based transhipment model for targeting the outsourced electricity requirements (Chen et al., 2013) and allocating renewable electricity and storage components to demands in hybrid power systems (Chen et al., 2014).

2. Proposed approach

This work proposes a novel approach for the identification of optimum PMSs in RES-based smart grids by using the Power Grand Composite Curves (PGCC) method to adaptively adjust the system operation in short-term power requirements. The main aim is to identify the optimum PMS within recurrent subsequent time intervals in order to minimize external non-RES utilization. The proposed approach builds on a generic smart grid model supporting the development of numerous different PMSs based on an inclusive representation of structural and temporal interactions.

2.1 Generic smart grid operating model

The key features of hybrid power generation smart grids involve conversion and accumulation of both material (Mt) and energy (Ng) flows at different time instants. In this context, regardless of equipment characteristics any smart grid may be described through interconnected converters (Cn) and accumulators (Ac) of an overall set $E=\{E^{Ac}, E^{Cn}\}$, processing flows at different states S of an overall set $S=\{S^{Ng}, S^{Mt}\}$, (Giaouris et al., 2013). The flows may be calculated as follows:

$$F_{t,n}^{In,j} = SF_{t,n}^{j} + \sum_{l}\left(\varepsilon_{t,l\to n} F_{t,l\to n}^{Out,j}\right) + \sum_{g}\left(\varepsilon_{t,g\to n} \cdot F_{t,g\to n}^{Out,j}\right) \tag{1}$$

where $l \in E^{Ac}, g \in E^{Cn}, n \in E, j \in S$, $F_{t,l\to n}^{Out,j}$ is the output flow of accumulator l directed to device n, in state j, $SF_{t,n}^{j}$ is a possible external signal or flow (e.g., solar radiation) and $\varepsilon_{t,l\to n}$ is a binary variable that becomes 1 when accumulator l feeds device n in state j. The same holds for converters. The accumulators are characterised by the amount of stored energy or material which can be defined as follows:

$$SOAcc_{t}^{l} = SOAcc_{t^-}^{l} + (F_{n\to l,t}^{in,j} - F_{l\to n,t}^{out,j}) / C_l \tag{2}$$

where $SOAcc_{t}^{l}$ is the amount of stored energy or material in accumulator l at time instant t, the symbol t^- is used to account for the previous observation instant and C_l is the total capacity of accumulator l. The investigated accumulators may store only one state hence symbol j is omitted for simplicity. To apply the above balance equations it is necessary to define variables ε of Eq. (1) as they enable the activation/deactivation of connections between devices m and n based on temporally evolving constraints. Variable $\varepsilon_{t,m\to n}$ can be defined in the form of a generic set of logical proposition as follows:

$$\varepsilon_{t,m\to n} = L\left(\varepsilon_{t,m\to n}^{Avl}, \varepsilon_{t,m\to n}^{Req}, \varepsilon_{t,m\to n}^{Gen}\right) \tag{3}$$

$$\varepsilon_{t,m\to n}^{i} = L_{m\to n}^{i}\left(L_{m\to n}^{SOAcc^l}\left(\rho_{t,m\to n}^{SOAcc^l}, r_{t,m\to n}^{SOAcc^l}\right)\right) \forall i = \{Avl, Req\}, n \in E^{Ac}, m \in E \tag{4}$$

In Eqs. (3)-(4) L is a logical operator and indices Avl and Req correspond to availability or requirement for material or energy as a condition for activation/deactivation of a device. Index Gen represents a free use of variable ε^{Gen} to incorporate any additional desired condition. Binary variables ρ and r are parameters associated with temporal conditions imposed on the power or materials stored in the accumulator l ($SOAcc^l$). Each converter m is activated/deactivated based on a $SOAcc^l$ value of each accumulator that controls it as follows:

$$\rho_{t,m\to n}^{SOAcc^l} = \left[SOAcc_t^l < Lo_{t,m\to n}^{SOAcc^l} \right] \vee \left[\left[Lo_{t,m\to n}^{SOAcc^l} < SOAcc_t^l < Up_{t,m\to n}^{SOAcc^l} \right] \wedge \left[\varepsilon_{t^-,m\to n} = 1 \right] \right] \quad (5)$$

In Eq. (5) terms Lo and Up refer to lower and upper limits in $SOAcc$. The first inequality represents the simple ON-OFF behaviour, while the subsequent expression represents the hysteresis behaviour (Giaouris et al., 2013). Hysteresis refers to activation/deactivation of converters based on their state in the previous instant (t^-). The recurring implementation of Eqs. (3)-(5) for a desired interval results in a PMS. Different PMSs result from different combinations of logical operators or values imposed on the upper and lower limits. Parameter r of Eq. (4) is used with ρ to impose or ignore a condition if necessary.

2.2 Adaptive management method

Let a hybrid renewable energy and storage grid system operating within an overall horizon time H divided into k equal time intervals and each interval is further divided into subintervals [t_0, T]. For example H can be a year that is divided into 365 days, i.e. $k\in[1, 365]$ and each day divided into intervals of 1h, i.e. t_0=1 and T=24. Also let a $PMS_{q,k} = f(\varepsilon_{k,t}, SOAcc_{k,t}^l)_q$ from a set of Q overall PMSs realized within an interval k (now added in all previous parameters) as any potential operating combination resulting from Eq(3)-(5). The proposed approach consists of the following main steps:

1. The PGCC of the system is developed at the subsequent time interval $k+1$ indicating the external non-RES input required to satisfy the power demand. An appropriate shift in the PGCC sets a target of the minimum power inventory needed by the end of the current interval k to completely avoid the use of non-RES power input in the subsequent interval.
2. The optimum PMS is selected in the current time interval k to meet the previously identified target by the end of this interval.

For the implementation of step 1 it is necessary to consider all possible PMSs at interval k+1 for the expected weather conditions and power demands. As shown in Figure 1a different PMSs result in different PGCCs and different outsourced electricity supply (OES) requirements for the system. For example, $PMS_{0,k+1}$ results in $SOAcc_{k+1,OES_0}^l > SOAcc_{k+1,OES_2}^l$ required with the use of $PMS_{2,k+1}$. Note that the OES for different PMSs may also be identified at different instants. Since the goal in step 1 is to develop a sufficient inventory in interval k so that the system may operate autonomously in interval k+1 (i.e. without the use of non-renewable resources) it is necessary to ensure that this goal is satisfied regardless of the PMS employed in interval k+1. This may only be achieved by testing $PMS_{q,k+1}$ for every $q \in Q$ and selecting the maximum $SOAcc_{k+1,OES_q}$. The latter will represent the minimum outsourced electricity supply (MOES) for the system, which will instead be provided as an energy inventory developed in interval k. This may be described by the following equations:

$$SOAcc_{k+1,Shift}^l = \max_{q\in Q} SOAcc_{k+1,OES_q}^l \quad (6)$$

$$SOAcc_{T,PMS_{targ,k}}^l = SOAcc_{t_0,PMS_{\max,k+1}}^l + SOAcc_{k+1,Shift}^l \quad (7)$$

Eq. (7) indicates the shift that needs to be implemented in the selected PGCC which is represented by $PMS_{\max,k+1}$ (Figure 1b). It also shows the amount of energy that needs to become available at $t=T$ in interval k. The subscript "max" used in Eq. (7) refers to the q^{th} PMS satisfying Eq(6). Notice that for implementation of Eq. (7), the PMS resulting in the selected $SOAcc_{k+1,Shift}^l$ may not allow the activation of converters which consume energy below the Pinch. In this context, the activation of the appropriate converter may be imposed through Eqs. (3)-(5). The subscript "*targ*" used in Eq. (7) refers to the PMS best matching the $SOAcc_{T,PMS_{targ,k}}^l$ target and remains to be identified at interval k in step 2. Also notice that the PMS required in order to match the shifted PGCC in this interval will be identified in a subsequent iteration using weather and demand data from interval k+2 (i.e. interval k+2 will become the new interval k+1 and so forth).

In order to implement step 2 it is necessary to consider all PMSs at interval k and find $PMS_{opt,k}$ so that:

$$\min_{q\in Q}(SOAcc_{T,PMS_{targ,k}} - SOAcc_{T,PMS_{q,k}}) \tag{8}$$

The procedure is illustrated in Figure 2 where the PGCC is shifted first in interval k+1 and then from implementation of Eqs. (6)-(7) it is found that $PMS_{opt,k}$= $PMS_{0,k}$. The correct way to read Figure 2 is from right to left. In the next iteration, the current interval k+1 becomes the new k and the procedure is repeated.

Eqs. (6) -(7) may take the following form to account for different potential limits and operating goals:

$$SOAcc^{l}_{k+1,Shift_h} = \left\{ \max_{q\in Q} SOAcc^{l}_{k+1,OES_q} \right\}_h \tag{9}$$

$$SOAcc^{l}_{T,PMS_{targ,k}} = SOAcc^{l}_{t_0,PMS_{\max,k+1}} + \sum_{h=1}^{N_{lm}} (c_h \cdot SOAcc^{l}_{k+1,Shift_h}) \quad \text{with} \sum_{h=1}^{N_{lm}} c_h = 1 \tag{10}$$

N_{lm} is the total number of limits imposed on $SOAcc$ depending on the considered converters (each limit determines when to activate/deactivate a converter). Note that during implementation of Eqs. (6)-(7) converters consuming power should be allowed to operate only above the Pinch. This may be imposed though Eqs. (3)-(5). Upper limits may be treated in the same way as lower limits. In such a case there would be a shift-down (instead of the shift-up of Figure 1b) to Pinch an upper limit, below a max $SOAcc$ level. The coefficient c_h determines the sign depending on energy is supply (i.e. Lower Level Pinch) or utilization (i.e. Upper Level Pinch). If c_h=1 the use of external sources is avoided through Eq. (8). If c_h=-1, Eq. (10) shows the energy that should be utilized before violation of an upper limit, indicating the undesired de-activation of a converter. If both limits are applicable the choice of c_h allows the prioritization of the actions. Eqs. (9)-(10) hold for N_{lm} = 2. In case of N_{lm} > 2 Eq. (11) is repeated depending on the shape of the PGCC.

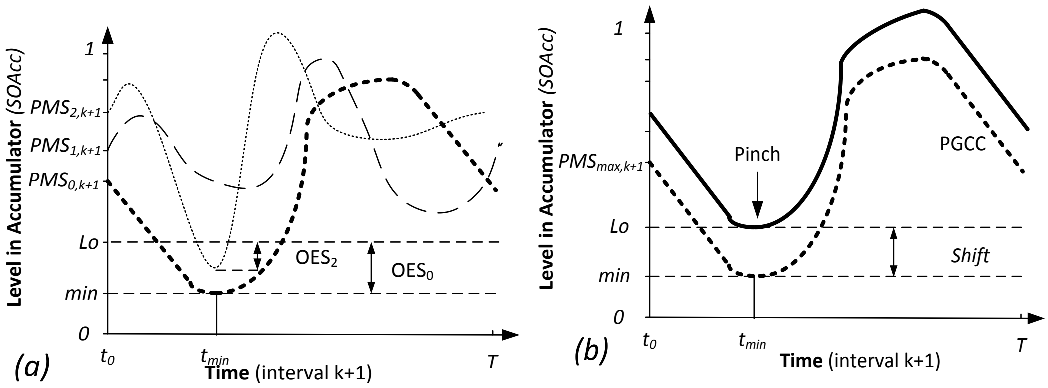

Figure 1: a) PGCCs for different PMSs, b) Pinch Point generated by shifted PGCC

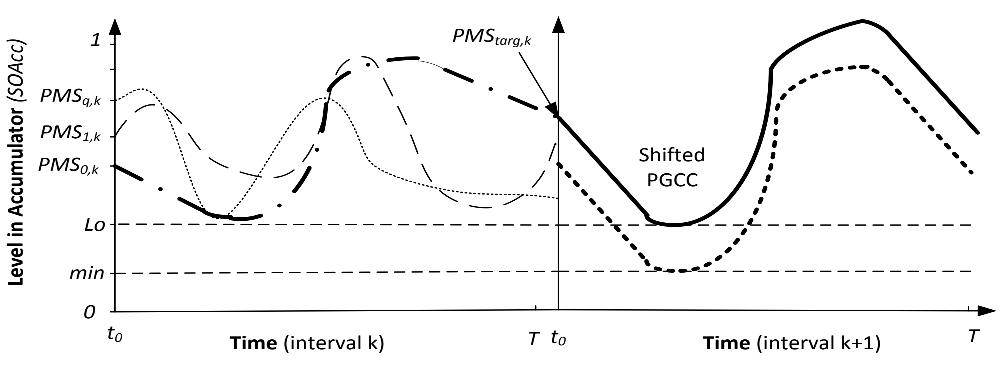

Figure 2: Matching of PGCCs from different PMSs between intervals k and k+1

3. Implementation

The considered hybrid smart grid consists of PV panels (PV) and wind generators (WG). Surplus energy is supplied to an electrolyzer (EL) after the specified load demand (LD) is satisfied. The produced H_2 is stored in pressurized cylinders (BT) and in cases of energy deficit, is utilized in a fuel cell (FC) to power the system. Lead-acid batteries (BAT) are used to regulate the power flows through frequent charging and discharging cycles induced by the RES variability. In case of energy excess, units such as the H_2 compressor (CP) utilize this energy to store H_2 in long-term storage tanks (FT). A diesel generator (DSL) is also utilized in cases of emergency (i.e. power demands of the application cannot be covered by RES or stored H_2). To illustrate the proposed method (considering space restrictions), it is applied for 2 PMS previously detailed in Giaouris et al. (2013). Both PMS activate the associated sub-systems as follows:

1. FC is activated ($\varepsilon^{Avl}_{t,FC\rightarrow BAT}$ =1) if $SOAcc^{BAT}_{t} < Lo^{SOAcc^{BAT}}_{t,FC\rightarrow BAT}$ and hysteresis is imposed until $Up^{SOAcc^{BAT}}_{t,FC\rightarrow BAT}$.
2. EL is activated ($\varepsilon^{\mathrm{Re}q}_{t,BAT\rightarrow EL}$ =1) if $SOAcc^{BAT}_{t} > Up^{SOAcc^{BAT}}_{t,BAT\rightarrow EL}$ and hysteresis is imposed until $Lo^{SOAcc^{BAT}}_{t,BAT\rightarrow EL}$.
3. DSL is activated if $SOAcc^{BAT}_{t} < Lo^{SOAcc^{BAT}}_{t,DSL\rightarrow BAT}$ and hysteresis is imposed until $Up^{SOAcc^{BAT}}_{t,DSL\rightarrow BAT}$.
4. PV is activated if $SOAcc^{BAT}_{t} < Lo^{SOAcc^{BAT}}_{t,PV\rightarrow BAT}$ without a hysteresis zone.
5. WG is activated if $SOAcc^{BAT}_{t} < Lo^{SOAcc^{BAT}}_{t,WG\rightarrow BAT}$ without a hysteresis zone.

While the above points are common between the two PMS, additional conditions differentiating the two PMSs are that $\varepsilon^{Gen}_{t,FC\rightarrow BAT} = 1$ if $\left[F^{Out,Pow}_{PV\rightarrow BAT} + F^{Out,Pow}_{WG\rightarrow BAT} - F^{Out,Pow}_{BAT\rightarrow LD} < 0\right]$ and $\varepsilon^{Gen}_{t.EL\rightarrow BF} = 1$ if $\left[F^{Out,Pow}_{PV\rightarrow BAT} + F^{Out,Pow}_{WG\rightarrow BAT} - F^{Out,Pow}_{BAT\rightarrow BAT} > 0\right]$ for PMS_2, while for PMS1 the two conditions don't apply

4. Results and discussion

The method is applied to find the PMS that avoids the activation of the DSL during two days considering local, hourly averaged weather data. The goal is to ensure that the $SOAcc^{BAT}$ remains above 0.2 (*Lo* limit) to satisfy a constant load of 2 kW. Initially the hysteresis zone of the FC is from 0.3 to 0.35 while for the DSL from 0.2 to 0.205. The initial $SOAcc$ was set at 0.3 for the BAT and 0.7 for the FT, BF and WT. The remaining parameters (e.g., size of BAT, FT and so forth) are described in Giaouris et al. (2013).

To find the optimum PMS in Day 1 we investigate the power generation profile of Day 2 considering the 2 PMSs. Eq. (6) indicates that the PMS resulting in the largest shift (i.e. in the minimum $SOAcc^{BAT}$ at t=$t_{\min}$ as shown in Figure 1) should be selected. However, each PMS may start from any possible $SOAcc^{BAT}$ at t=0, whereas different values of $SOAcc^{BAT}$ at t=0 may also result in identical values of $SOAcc^{BAT}$ at t=$t_{\min}$. It is necessary to identify those $SOAcc^{BAT}$ values (at t=0) prior to implementing Eq(6). Using a step size of 0.001 we calculate the estimated PGCC for all values of $SOAcc^{BAT}$ from 0.2 to 0.8 for both PMS (in Day 2). This generates 1,200 PGCC graphs which indicate 3 initial values (i.e. $SOAcc^{BAT}$ at t=0) for PMS_1 and 2 for PMS_2. These are shown in Table 1 and illustrated in Figure 3b with different lines for PMS_1. The highest value is selected as $SOAcc^{BAT}$ at t=0 for each PMS, ensuring that the resulting curve will not violate the *Lo* limit. The shift in the PGCC of PMS_1 and PMS_2 to Pinch at the *Lo* limit is 0.016 and 0.007 (Table1). Based on Eq. (6) the selected PGCC (i.e. $PMS_{\max,k+1}$) corresponds to PMS_1 and the $SOAcc^{BAT}$ (at t=$t_{\min}$) is shifted by 0.016 in order to Pinch the limit of 0.2. Based on Eq. (7) the targeted $SOAcc^{BAT}$ for Day 1 should be at 0.241. Hence if for PMS_1 the initial $SOAcc^{BAT}$ is 0.241 and the operating regions of DSL and FC are also shifted by 0.016 we can be sure that regardless of PMS the $SOAcc^{BAT}$ will not drop below 0.2.

Therefore the chosen PMS for Day 1 is the one that will generate a final value of the $SOAcc^{BAT}$ as close to 0.241 as possible, based on Eq. (8). The latter is the level of charge that should be stored in the battery in Day 1 in order to avoid using the DSL in Day 2. Again it is possible to calculate the PGCC for Day 1 and

Table 1: *$SOAcc^{BAT}$ values considered in the case study*

$SOAcc^{BAT}$	PMS_1	PMS_2
Minimum limit (*min*)	0.184	0.193
Lower limit (*Lo*)	0.2	0.2
Shift	0.2-0.184=0.016	0.2-0.193=0.007
Initial	0.201, 0.209, 0.225	0.208, 0.232
Targeted (*targ*)	0.225+0.2-0.184=0.241	0.232+0.2-0.193=0.239

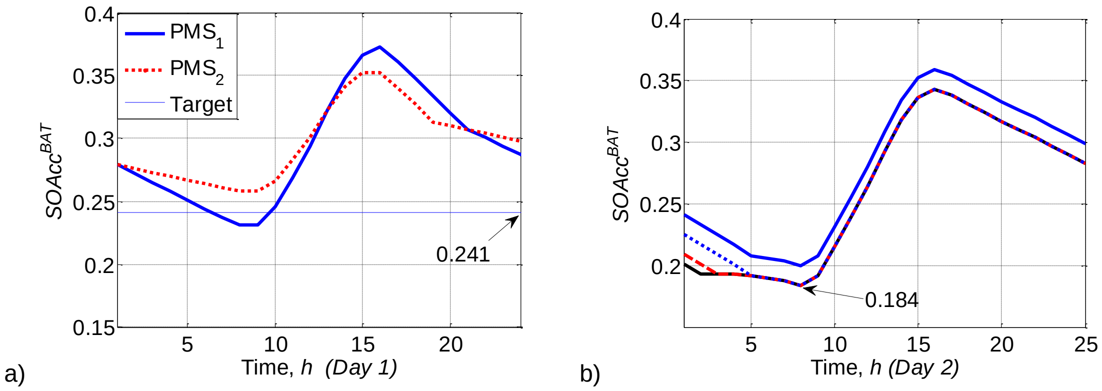

Figure 3: a) PGCC curves for Day 1 for PMS_1 and PMS_2, b) Initial and shifted PGCC for PMS_1 in Day 2

starting from the given initial conditions (0.3 for BAT and 0.7 for the other accumulators) we see that PMS_1 will produce the best result and a final $SOAcc^{BAT}$ at 0.2790 while the FT will be at 0.561. Repeating for Day 2, we focus on Day 3 and PMS_1 produces a $SOAcc^{BAT}$ (at t=$t_{\min}$) of 0.194 for initial $SOAcc^{BAT}$ at 0.229 imposing a shift at 0.235. The chosen PMS for Day 2 is again PMS_1, producing a final $SOAcc^{BAT}$ at 0.28.

5. Conclusions

The use of the PGCC method was presented as formal and generic mathematical formulations supporting the graphical tools and facilitating the recursive implementation of the method for long time horizons. Although the presented case study considered daily time intervals, the proposed method may be implemented for shorter time intervals. This is very important because the potential combination of the method with short-term weather forecasts could enable a very efficient adaptation of the system in view of variable weather conditions. As this is on-going work, more extensive case studies are developed addressing multiple PMS. Additional power management scenarios are investigated including cases of simultaneously satisfying multiple operating goals or multiple Pinches.

Acknowledgement

Funding from NSRF 2007-2013 (GR and EU) program “SYNERGASIA” (09SYN-32-594) is acknowledged.

References

Bandyopadhyay S., 2011, Design and optimization of isolated energy systems through pinch analysis, Asia-Pac. J. Chem. Eng., 6, 518-526.

Chen C.L., Lai C.T., Lee J.Y., 2014, Transshipment model-based MILP (mixed-integer linear programming) formulation for targeting and design of hybrid power systems, Energy, 65, 550-559.

Chen C.L., Lai C.T., Lee J.Y., 2013, A process integration technique for targeting and design of off-grid hybrid power networks, Chem. Eng. Trans., 35, 499-504.

Giaouris D., Papadopoulos A.I., Ziogou C., Ipsakis D., Voutetakis S., Papadopoulou S., Seferlis P., Stergiopoulos F., Elmasides C., 2013, Performance investigation of a hybrid renewable power generation and storage system using systemic power management models, Energy, 61, 621-635.

Ho W.S., Khor C.S., Hashim H., Macchietto S., Klemeš J.J., 2013, SAHPPA: a novel power pinch analysis approach for the design of off-grid hybrid energy systems. Clean Technol. Envir. Policy, 16(5), 957-970

Klemeš J.J., Ed, 2013, Process Integration Handbook, Woodhead/Elsevier, Cambridge, UK

Rozali N.E.M., Wan Alwi S.R., Manan Z.A., Klemeš J.J., Hassan M.Y., 2013a, Optimisation of pumped-hydro storage system for hybrid power system using power pinch analysis, Chem Eng Trans, 35, 85-90.

Rozali N.E.M., Wan Alwi S.R., Manan Z.A., Klemeš J.J., Hassan M.Y., 2013b, Optimal sizing of hybrid power systems using power pinch analysis, J. Clean. Prod., 71, 158-167.

Rozali N.E.M., Wan Alwi S.R., Manan Z.A., Klemeš J.J., Hassan M.Y., 2013, Process integration techniques for optimal design of hybrid power systems, Appl. Therm. Eng., 61,26-35.

Wan Alwi S.R., Rozali N.E.M., Manan Z.A., Klemeš J.J., 2012a, A process integration targeting method for hybrid power systems, Energy, 44, 6-10.

Wan Alwi S.R., Rozali N.E.M., Manan Z.A., Klemeš J.J., 2012b, Design of hybrid power systems with energy losses, Chem. Eng. Trans., 29, 121-126.